Alexandria Engineering Journal (2016) 55, 635–644

HOSTED BY

ELSEVIER

Alexandria University

Alexandria Engineering Journal

www.elsevier.com/locate/aej
www.sciencedirect.com

Transient hydromagnetic reactive Couette flow and heat transfer in a rotating frame of reference

S. Das [a,*], R.N. Jana [b], O.D. Makinde [c]

[a] *Department of Mathematics, University of Gour Banga, Malda 732 103, India*
[b] *Department of Applied Mathematics, Vidyasagar University, Midnapore 721 102, India*
[c] *Faculty of Military Science, Stellenbosch University, Private Bag X2, Saldanha 7395, South Africa*

Received 9 May 2015; revised 11 November 2015; accepted 5 December 2015
Available online 4 January 2016

KEYWORDS

Hydromagnetic;
Couette flow;
Reactive fluid;
Heat transfer

Abstract This paper is concerned with the study of a transient hydromagnetic Couette flow and heat transfer of a reactive viscous incompressible electrically conducting fluid between two infinitely long horizontal parallel plates when one of the plate is set into uniform accelerated motion in the presence of a uniform transverse magnetic field under Arrhenius reaction rate. The transient momentum equations are solved analytically using the Laplace transform technique and the velocity field and shear stresses are obtained in a unified closed form. The energy equation is tackled numerically using MATLAB. The effects of the pertinent parameters on the fluid velocity, temperature, the shear stress and the rate of heat transfer at the plates are presented in graphical form and discussed in detail. Our results reveal that the combined effects of magnetic field, rotation, exothermic reaction and variable thermal conductivity have significant impact on the hydromagnetic flow and heat transfer.

1. Introduction

In fluid dynamics, Couette flow refers to the laminar flow of a viscous incompressible fluid in the space between two parallel plates, one of which is moving and the other remains fixed. Couette flow occurs in fluid machinery involving moving parts and is especially important for hydrodynamic lubrication. Couette flow has been used as the fundamental method for the measurement of viscosity and as a means of estimating the drag force in many wall driven applications [1]. Magnetohydrodynamic (MHD) is concerned with the mutual interaction of conducting fluid flow and magnetic field. The fluids being investigated must be electrically conducting, which limits the fluids to liquid metals, hot ionized gases (plasmas) and strong electrolytes. The study of magnetic field effects has considerable interest in the technical fields due to its applications in industrial technology. These applications include MHD power generators, cooling of nuclear reactors, liquid metal flow control, micro MHD pumps, high-temperature plasmas, biological transportation, drying processes and solidification of binary alloy. Moreover, recent findings on magnetohydrodynamics have shown that the magnetic field produced by a simple magnet placed in a transverse direction to the channel does interact with the fluid flow and plays important role in

* Corresponding author. Tel.: +91 3222 261171.
E-mail addresses: jana261171@yahoo.co.in, tutusanasd@yahoo.co.in (S. Das).

Peer review under responsibility of Faculty of Engineering, Alexandria University.

http://dx.doi.org/10.1016/j.aej.2015.12.009

the control of hot moving fluid in many metallurgical engineering applications, crystal growth, electrochemistry and other thermal processes occurring at high temperature.

In many geophysical and industrial energy system flows, the effects of the Coriolis force have a significant influence on the fluid dynamics of the system. It has been widely demonstrated, for example, that the hydromagnetic flow in the earth's liquid core generates the main geomagnetic field. Coriolis and hydromagnetic forces in this context are of the same order of magnitude. The interplay of these two forces is therefore of great interest in magnetohydrodynamics. Rotating MHD generators are also an area of primary applications. Due to vast applications of magnetic fields in conjunction with rotational effects in modern material processing such as stabilization of thin magnetic liquid films and homogeneity control of conducting fluids, many researchers have been interested in the study of MHD flows in rotating systems. Fluid flows under the influence of applied magnetic field are apparent in certain engineering processes such as glass manufacturing, paper production, polymer technology, plasma studies, geothermal energy extraction, ionized-geothermal energy systems, the boundary layer control in the field of aerodynamics and blood flow problems. Meanwhile, hydromagnetic flow and heat transfer have received considerable attention in recent years due to its various applications in science, engineering and industries. Furthermore, hydromagnetic flow in a rotating environment has received significant attention of several researchers due to its applications in various technological situations which are governed by the action of Coriolis force. Oceanography, meteorology, atmospheric science and limnology all contain some important and essential features of rotating fluids. An order of magnitude analysis shows that in basic field equations the effects of Coriolis force are more significant as compared to those of inertia and viscous forces. It is worthy to note that Coriolis and magnetohydrodynamic forces are comparable in magnitude and Coriolis force induces secondary flow in the fluid. Several excellent studies have been presented concerning rotating hydromagnetic flows for various geometrical situations including channels, plates, spheres, disks. Nanda and Mohanty [2] studied the hydromagnetic flow in a rotating channel. Jana et al. [3] presented the magnetohydrodynamic Couette flow and heat transfer in a rotating system. Hall effects on MHD Couette flow in a rotating system were examined by Jana and Datta [4]. An unsteady hydromagnetic Couette flow in a rotating system was presented by Seth et al. [5]. An MHD Couette flow and heat transfer in a rotating system was presented by Seth and Maiti [6]. Seth and Ghosh [7] examined the Hall effects on an unsteady hydromagnetic flow in a rotating channel with oscillating pressure gradient. Chandran et al. [8] examined the effect of rotation on an unsteady hydromagnetic Couette flow. Singh et al. [9] studied the magnetohydrodynamic Couette flow with rotation. Das et al. [10] studied an unsteady MHD Couette flow in a rotating system. Gosh et al. [11] examined the Hall effects on an MHD flow in a rotating system with heat transfer. An unsteady hydromagnetic Couette flow induced due to accelerated movement of one of the porous plates of the channel in a rotating system was presented by Seth et al. [12]. The combined effects of Hall and ion-slip currents on an unsteady MHD Couette flows in a rotating system were examined by Jha and Apere [13]. Jha and Apere [14] presented an MHD Couette flow in a rotating system with suction/injection. Bég et al. [15] studied the magnetohydrodynamic flow in rotating porous media taking Hall currents and inclined magnetic field influence. Das et al. [16] examined the effects of Hall currents on an MHD Couette flow in rotating system. Jha and Apere [17] presented an MHD Couette flow of rotating fluid with Hall and ion-slip currents. Singh and Pathak [18] examined the effect of rotation and Hall currents on a mixed convection MHD flow through a porous medium filled in a vertical channel in the presence of thermal radiation. Chauhan and Agrawal [19] examined effects of Hall current on MHD Couette flow in a channel partially filled with a porous medium in a rotating system. Seth and Singh [20] examined effects of Hall currents on an unsteady MHD Couette flow of class - II in a rotating system. An unsteady rotating hydromagnetic free and forced convection in a channel subject to forced oscillation under an oblique magnetic field was described by Ghosh et al. [21]. Recently, Seth et al. [22] have studied an unsteady hydromagnetic natural convection flow of a heat absorbing fluid within a rotating vertical channel in porous medium with Hall effects. Seth and Singh [23] have described the mixed convection hydromagnetic flow in a rotating channel with Hall and wall conductance effects.

Almost all the above mentioned studies have assumed that fluid properties are constant. However experiments indicate that this can only hold, if temperature does not change rapidly or impulsively in any particular way. Hence more accurate prediction of flow and heat transfer can only be obtained by considering variations of fluid and electromagnetic properties, especially variations of fluid viscosity, thermal conductivity as well as electrical conductivity with temperature. The study of reactive viscous fluids under a Couette flow scenario in a rotating system is extremely important in understanding lubricant hydrodynamics and heat transfer in engineering and industrial systems. Generally speaking, most lubricants used in both engineering and industrial processes are reactive e.g. hydrocarbon oils, polyglycols, synthetic esters, and polyphenylethers and their efficiency depends largely on the temperature variation from time to time. It is thus important to determine the heat transfer conditions and thermal loading properties of viscous reactive fluids to gauge their effectiveness as lubricants. Makinde [24] presented a steady flow of a reactive variable viscosity fluid in a cylindrical pipe with an isothermal wall. The second law analysis of Couette flow of a reactive fluid with variable viscosity under Arrhenius kinetics was carried out by Kobo and Makinde [25]. Makinde and Onyejekwe [26] studied an MHD generalized Couette flow and heat transfer with variable viscosity and electrical conductivity. Chinyoka and Makinde [27] studied the transient generalized Couette flow of a reactive third-grade liquid with asymmetric convective cooling. Theuri and Makinde [28] presented the thermodynamic analysis during MHD unsteady generalized Couette flow of viscous fluid with variable viscosity. The thermal analysis of a reactive generalized Couette flow of power law fluids between concentric cylindrical pipes was provided by Makinde [29]. Makinde and Franks [30] studied an MHD unsteady reactive Couette flow with heat transfer and variable properties. Recently, an unsteady MHD free convective Couette flow with thermal radiation has been studied by Jha et al. [31]. Jha et al. [32] have obtained the exact solution of a fully developed MHD natural convection flow in a vertical annular microchannel. Nayak and Dash [33] have studied the magnetohydrodynamic couple stress fluid flow through a porous medium in a rotating channel.

Our present paper is devoted to examine the combined effects of rotation and the magnetic field on the transient hydromagnetic Couette flow of a reactive viscous incompressible electrically conducting fluid between infinite horizontal parallel plates in a rotating system. The momentum governing equations are solved analytically by employing the Laplace transform technique. It is assumed that conducting incompressible fluid is subjected to an exothermic reaction under Arrhenius kinetics, neglecting the consumption of the material. The effects of the pertinent parameters on the fluid velocity, temperature, shear stress and heat transfer rate are discussed with the help of graphs and tables.

2. Formulation of the problem and its solution

Consider the unsteady MHD flow of a viscous incompressible electrically conducting fluid between two infinite horizontal parallel plates when the fluid and the plates rotate in unison with uniform angular velocity Ω about an axis normal to the plates. Let h be the distance between the two plates.

The upper plate moves with a velocity $U(t)$ which is a known function of time t in its own plane in the x-direction, where the x-axis is taken along the lower stationary plate in the direction of the flow. The y-axis is taken normal to the x-axis and the z-axis is taken normal to the xy-plane (see Fig. 1), lying in the plane of the lower plate. A uniform transverse magnetic field of strength B_0 is applied in the positive y-direction. Initially, at time $t \leqslant 0$, the two plates and the fluid are assumed to be at the same temperature T_0 and stationary. At time $t > 0$, the plate at $y = h$ starts to move in its own plane with the velocity $U(t)$ and its temperature is T_0 whereas the plate at $y = 0$ is stationary and maintained at a constant temperature T_0. Since the plates are infinitely long along the x- and z-directions, all physical quantities will be functions of y and t only.

It is assumed that induced magnetic field produced by the fluid motion is negligible in comparison with the applied one so that we take magnetic field as $\vec{B} = (0, 0, B_0)$. This assumption is justified because magnetic Reynolds number is generally very small for metallic liquids and partially ionized fluids [34]. Liquid metals can be used in a range of applications because they are nonflammable, nontoxic and environmentally safe. That is why, liquid metals have number of technical applications in source exchangers, electronic pumps, and ambient heat exchangers and also used as a heat engine fluid. Moreover, in nuclear power plants sodium, alloys, lead–bismuth and bismuth are extensively utilized as heat transfer fluids. Besides

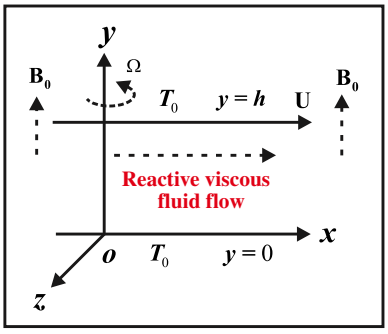

Figure 1 Geometry of the problem.

that, mercury plays its role as a fluid in high-temperature Rankine cycles and also used in reactors in order to reduce the temperature of the system. For power plants that are exerted at extensively high temperature, sodium is treated as heat-engine fluid. Also no external electric field is applied so the effect of polarization of fluid is negligible [34], so we assume $\vec{E} = (0, 0, 0)$. Under the above assumptions, the Navier–Stokes equations of motion in a rotating frame of reference are

$$\frac{\partial u}{\partial t} + 2\Omega w = -\frac{1}{\rho}\frac{\partial p}{\partial x} + \nu\frac{\partial^2 u}{\partial y^2} - \frac{\sigma B_0^2}{\rho}u, \tag{1}$$

$$0 = -\frac{1}{\rho}\frac{\partial p}{\partial y}, \tag{2}$$

$$\frac{\partial w}{\partial t} - 2\Omega u = -\frac{1}{\rho}\frac{\partial p}{\partial z} + \nu\frac{\partial^2 u}{\partial y^2} - \frac{\sigma B_0^2}{\rho}w, \tag{3}$$

where u and w are the fluid velocity components along x and z-directions respectively, ρ is the fluid density, ν is the kinematic viscosity, σ is the electrical conductivity and p is the fluid pressure. Eqs. (1)–(3) describe the hydromagnetic Couette flow between infinite horizontal parallel plates of any conducting medium due to the motion of the upper plate in a rotating system.

The initial and boundary conditions are

$$\begin{aligned} &t \leqslant 0: \ u = w = 0 \quad \text{for } 0 \leqslant y \leqslant h, \\ &t > 0: \ u = 0, \quad w = 0 \text{ at } y = 0 \text{ and } u = U(t), \\ &\quad w = 0 \text{ at } y = h. \end{aligned} \tag{4}$$

On the use of the boundary condition at $y = h$ and Eqs. (1) and (3), we have

$$\frac{\partial U}{\partial t} = -\frac{1}{\rho}\frac{\partial p}{\partial x} - \frac{\sigma B_0^2}{\rho}U, \quad -2\Omega U = -\frac{1}{\rho}\frac{\partial p}{\partial z}, \tag{5}$$

On the use of (5), the momentum Eqs. (1) and (2) along x- and z-directions become

$$\frac{\partial u}{\partial t} + 2\Omega w = \frac{\partial U}{\partial t} + \nu\frac{\partial^2 u}{\partial y^2} - \frac{\sigma B_0^2}{\rho}(u - U), \tag{6}$$

$$\frac{\partial w}{\partial t} - 2\Omega(u - U) = \nu\frac{\partial^2 u}{\partial y^2} - \frac{\sigma B_0^2}{\rho}w, \tag{7}$$

Introducing non-dimensional variables

$$\eta = \frac{y}{h}, \quad (u_1, w_1) = \frac{(u, w)}{u_0}, \quad \tau = \frac{\nu t}{h^2}, \quad U = u_0 f(\tau), \tag{8}$$

Eqs. (6) and (7) become

$$\frac{\partial u_1}{\partial \tau} + 2K^2 w_1 = \frac{\partial f}{\partial \tau} + \frac{\partial^2 u_1}{\partial \eta^2} - M^2(u_1 - f), \tag{9}$$

$$\frac{\partial w_1}{\partial \tau} - 2K^2(u_1 - f) = \frac{\partial^2 w_1}{\partial \eta^2} - M^2 w_1, \tag{10}$$

where $M^2 = \frac{\sigma B_0^2 h^2}{\rho\nu}$ is the magnetic parameter representing the ratio of electromagnetic (Lorentz) force to the viscous force, $K^2 = \frac{\Omega h^2}{\nu}$ the rotation parameter which is the ratio of Coriolis force to the viscous force i.e. inversely proportional to Ekman number. Large values of Ekman number imply lesser rotational effects. Typical geophysical flows and also laboratory experiments yield very small Ekman numbers. A small value of the Ekman number indicates that vertical friction plays a

very minor role in the balance of forces and may, consequently, be omitted. For $K^2 = 1$, the viscous and rotational forces are of the same order of magnitude. For $K^2 > 1$, the rotational effects clearly dominate viscous effects. For $K^2 < 1$, the rotational effects are dominated by viscous effects.

The initial and boundary conditions (4) become

$$\begin{aligned}&\tau \leqslant 0: \ u_1 = w_1 = 0 \text{ for } 0 \leqslant \eta \leqslant 1,\\ &\tau > 0: \ u_1 = 0, \quad w_1 = 0 \text{ at } \eta = 0 \text{ and } u_1 = f(\tau),\\ &\quad w_1 = 0 \text{ at } \eta = 1. \end{aligned} \tag{11}$$

Combining Eqs. (9) and (10), we get

$$\frac{\partial q}{\partial \tau} - 2iK^2 q = \frac{\partial^2 q}{\partial \eta^2} - M^2 q, \tag{12}$$

where $q = u_1 + iw_1 - f$ and $i = \sqrt{-1}$.

The initial and boundary conditions for $q(\eta, \tau)$ are

$$\begin{aligned}&\tau \leqslant 0: \ q = 0 \text{ for } 0 \leqslant \eta \leqslant 1,\\ &\tau > 0: \ q = -f \text{ at } \eta = 0 \text{ and } q = 0 \text{ at } \eta = 1. \end{aligned} \tag{13}$$

Taking the Laplace transform of Eq. (12) and on the use of (13), we have

$$s\bar{q} - 2iK^2\bar{q} = \frac{d^2\bar{q}}{d\eta^2} - M^2\bar{q}. \tag{14}$$

The boundary conditions for $\bar{q}(\eta, s)$ are

$$\bar{q}(0, s) = -\bar{f}(s) \text{ and } \bar{q}(1, s) = 0, \tag{15}$$

where $\bar{f}(s)$ is the Laplace transform of $f(\tau)$.

Solutions of Eq. (14) subject to the boundary conditions (15) are given by

$$\bar{q}(\eta, s) = -\bar{f}(s)\frac{\sinh\sqrt{a+s}(1-\eta)}{\sinh\sqrt{a+s}}, \tag{16}$$

where $a = M^2 - 2iK^2$.

The upper plate has been set into motion with a speed $f(\tau) = \tau$, which corresponds to the accelerated motion. Then the inverse Laplace transforms of Eq. (16) gives the solution for the velocity components as

$$\begin{aligned} u_1 + iw_1 = \tau - \tau\frac{\sinh(\alpha - i\beta)(1-\eta)}{\sinh(\alpha - i\beta)} + \frac{1}{2(\alpha - i\beta)\sinh^2(\alpha - i\beta)}\\ \times [\cosh(\alpha - i\beta)\sinh(\alpha - i\beta)(1-\eta) - (1-\eta)\\ \times \sinh(\alpha - i\beta)\cosh(\alpha - i\beta)\eta]\\ + 2\sum_{n=1}^{\infty}(-1)^n n\pi e^{-\{(\alpha - i\beta)^2 + n^2\pi^2\}\tau}\sin n\pi\eta, \end{aligned} \tag{17}$$

where $\alpha, \beta = \frac{1}{\sqrt{2}}\left[\left(M^4 + 4K^4\right)^{1/2} \pm M^2\right]^{1/2}$. Eq. (17) represents the general solution for the unsteady uniformly accelerated-started hydromagnetic Couette flow in a rotating system when the magnetic lines of force being fixed relative to the fluid. On separating into a real and imaginary parts one can easily obtain the velocity components u_1 and w_1 from Eq. (17). In the inertial frame of reference ($K^2 = 0$), the present problem reduces to the problem studied by Makinde and Franks [30].

3. Results and discussion

In order to have a physical insight into the problem, a parametric study is performed and the obtained numerical results are elucidated with the help of graphical illustrations. We have presented the non-dimensional fluid velocity components u_1 and w_1 for several values of magnetic parameter M^2, rotation parameter K^2 and time τ are presented in Figs. 2–6. The case $M^2 = 0$ corresponds to the absence of magnetic field. The default values of the other parameters are mentioned in the description of the respective figures.

3.1. Effects of parameters on primary and secondary velocity profiles

Figs. 2 and 3 show the time evolution of the primary and secondary velocity profiles across the channel for a fixed set of parameter values. The primary velocity and secondary velocity increase from its zero value at the lower fixed plate to its maximum value at the upper moving plate.

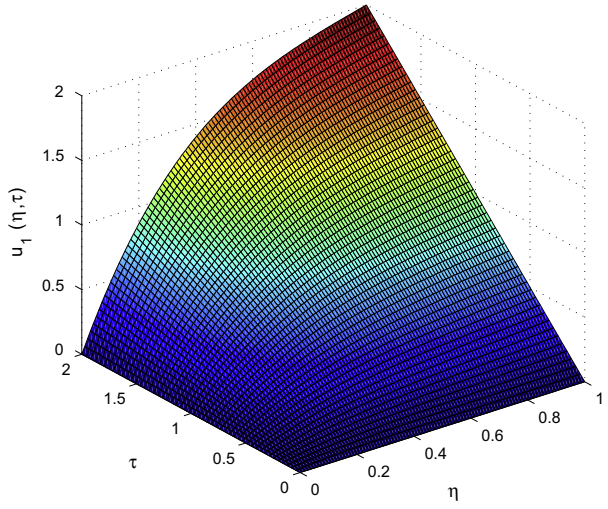

Figure 2 Primary velocity profiles across the channel with increasing time when $M^2 = 2$ and $K^2 = 4$.

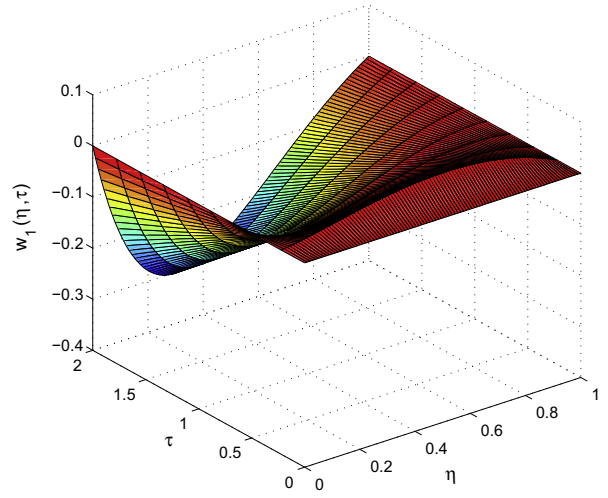

Figure 3 Secondary velocity profiles across the channel with increasing time when $M^2 = 2$ and $K^2 = 4$.

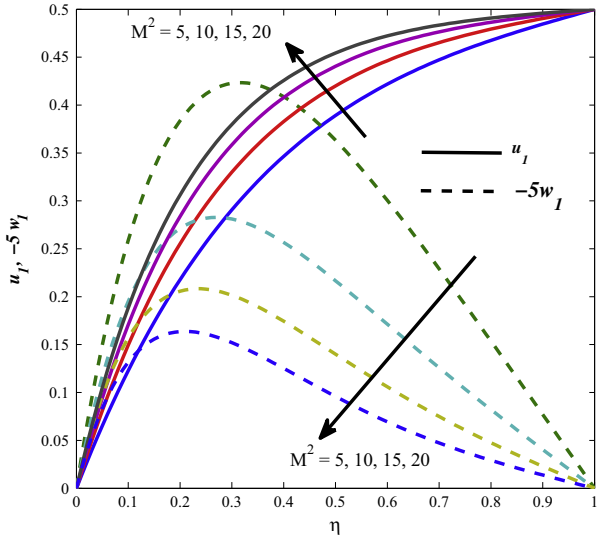

Figure 4 Primary and secondary velocity profiles for different M^2 when $K^2 = 4$ and $\tau = 0.5$.

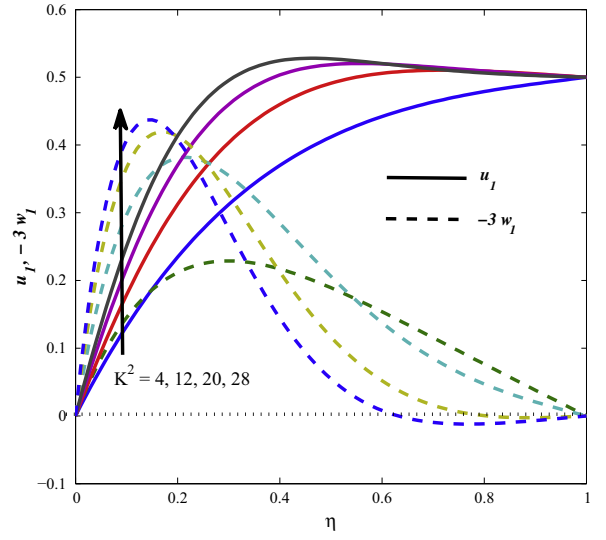

Figure 5 Primary and secondary velocity profiles for different K^2 when $M^2 = 5$ and $\tau = 0.5$.

It is seen from Fig. 4 that the primary velocity u_1 enhances and the magnitude of the secondary velocity w_1 retards for increasing values of magnetic parameter M^2. This is mainly due to the influence of Lorentz forces present in the magnetic field. This is an established result reported by many authors. Fig. 5 shows that the primary velocity u_1 increases and the magnitude of the secondary velocity w_1 enhances near the stationary plate and retards near the moving plate with an increase in rotation parameter K^2. This is because the Coriolis force exists only in rotating phenomena and this force produces the secondary velocity in flow field. In physics, the Coriolis effect is a deflection of moving objects in a rotating frame in the opposite direction. Also, the magnitude of the secondary velocity w_1 retards near the moving plate. It can be interpreted that the viscous force increases for the accelerated motion of the upper plate. Rotation acts to enhance secondary flow reversal closer to the moving plate. Close to the stationary plate, the primary velocity remains positive; further from the stationary plate, as we approach the channel center and thereafter the moving plate, there is a considerable retardation on the flow leading to significant flow reversal i.e. backflow. Backflow is maximized in the region of the upper channel half space in the vicinity of the moving plate for high rotation, i.e. $K^2 = 28$. The negative values of secondary velocity w_1 in Figs. 2–5 indicate that for counterclockwise sense of rotation Ω, the secondary velocity w_1 is in the clockwise sense relative to the direction of the primary flow. Therefore, the high rotation, i.e. dominance of Coriolis force over hydrodynamic viscous force is counterproductive for the stability of the secondary flow. One striking feature of the secondary velocity profile is marked in the case of high rotation, which provides a practical application in hydro magnetic rotating energy generator followed by Nayak and Dash [33].

3.2. Effects of parameters on shear stresses

For purposes of engineering design, the shear stresses at the channel plates are important. The non-dimensional shear stresses at the channel plates $\eta = 0$ and $\eta = 1$ are respectively given by

$$\tau_{x_0} + i\tau_{z_0} = \left[\frac{\partial}{\partial\eta}(u_1 + iw_1)\right]_{\eta=0} = \tau(\alpha - i\beta)\coth(\alpha - i\beta) + \frac{1}{2(\alpha - i\beta)\sinh^2(\alpha - i\beta)}[\cosh(\alpha - i\beta)\sinh(\alpha - i\beta) - (\alpha - i\beta)] + 2\sum_{n=0}^{\infty}(-1)^n n^2\pi^2 e^{-\{(\alpha - i\beta)^2 + n^2\pi^2\}\tau}, \quad (18)$$

$$\tau_{x_1} + i\tau_{z_1} = \left[\frac{\partial}{\partial\eta}(u_1 + iw_1)\right]_{\eta=1} = \tau(\alpha - i\beta)\mathrm{cosech}(\alpha - i\beta) + \frac{1}{2(\alpha - i\beta)\sinh^2(\alpha - i\beta)}[\sinh(\alpha - i\beta) - (\alpha - i\beta) \times \cosh(\alpha - i\beta)] + 2\sum_{n=0}^{\infty} n^2\pi^2 e^{-\{(\alpha - i\beta)^2 + n^2\pi^2\}\tau}, \quad (19)$$

We can then obtain the shear stresses at the plates due to the primary and the secondary flows on separating into real and imaginary parts of the complex Eqs. (18) and (19). Numerical results of the non-dimensional shear stresses τ_{x_0} and τ_{z_0} at the lower plate $\eta = 0$ due to the primary and the secondary flows and the shear stresses τ_{x_1} and τ_{z_1} at the upper plate $\eta = 1$ due to the primary and the secondary flows are presented in Figs. 6–9 for several values of magnetic parameter M^2, rotation parameter K^2 and time τ. Fig. 6 shows that the shear stress τ_{x_0} and the magnitude of the shear stress τ_{z_0} enhance for increasing values of rotation parameter K^2. This is because the rotational drag force leads to an increase in the fluid velocity gradient at both plate surfaces.

On other hand, the shear stress τ_{x_0} increases whereas the magnitude of the shear stress τ_{z_0} decreases as M^2 increases. As the magnetic field intensity increases, the velocity gradient increases at the lower fixed plate and decreases at the upper moving plate due to the resistance effect of Lorenz force at the upper plate. Fig. 7 reveals that the shear stress τ_{x_1} first decreases, reaches a minimum and then increases and the

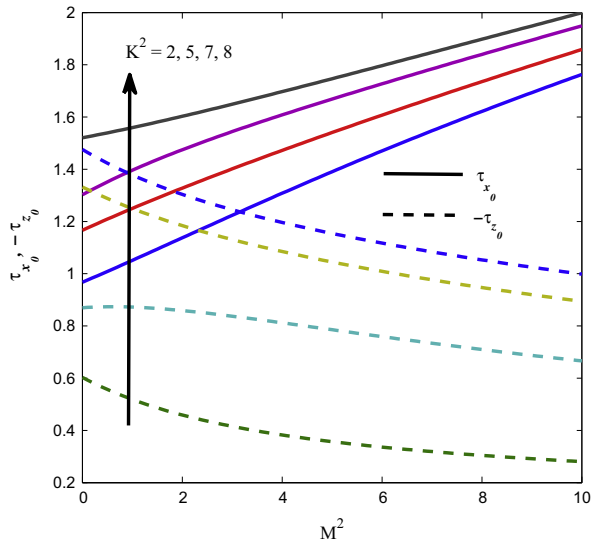

Figure 6 Shear stresses τ_{x_0} and τ_{z_0} for different K^2 when $\tau = 0.5$.

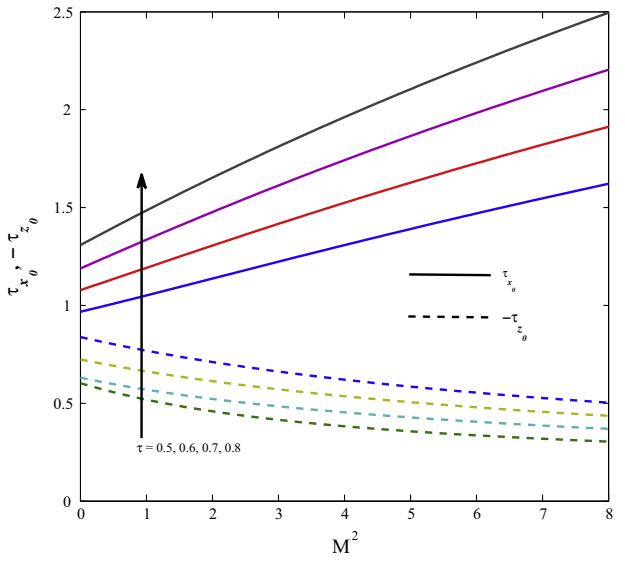

Figure 8 Shear stresses τ_{x_0} and τ_{z_0} with increasing time when $K^2 = 4$.

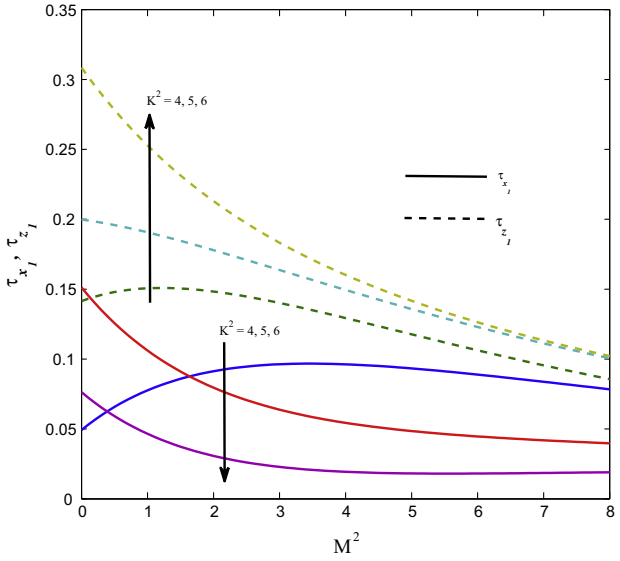

Figure 7 Shear stresses τ_{x_1} and τ_{z_1} for different K^2 when $\tau = 0.5$.

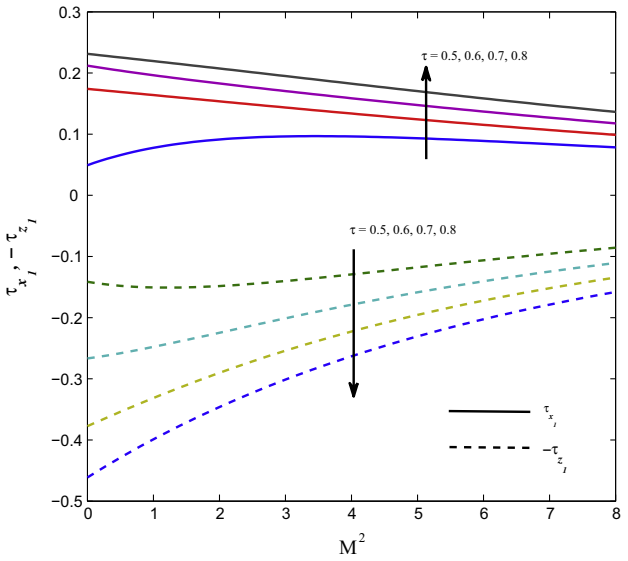

Figure 9 Shear stresses τ_{x_1} and τ_{z_1} with increasing time when $K^2 = 4$.

magnitude of the shear stress τ_{z_1} increases for increasing values of rotation parameter K^2. The positive values of the shear stress τ_{z_1} at the moving plate $\eta = 1$ due to the secondary flow actually confirm the existence of a backflow for the secondary velocity. The shear stress τ_{x_0} and the magnitude of the shear stress τ_{z_0} enhance when time τ progresses as shown in Fig. 8. As expected, a progress in time the velocity components is boosted up, leading to an increase in the shear stresses at the lower plate. On other hand, the shear stress τ_{x_0} increases whereas the shear stress τ_{x_0} decreases as time τ increases. Fig. 9 reveals that the shear stress τ_{x_1} increases whereas the magnitude of the shear stress τ_{z_1} decreases when time τ progresses. The flow separation does not occur as shear stresses are never zero.

3.3. Heat transfer

The energy equation taking viscous and Joule dissipations into account is given by

$$\rho c_p \frac{\partial T}{\partial t} = \frac{\partial}{\partial y}\left(k\frac{\partial T}{\partial y}\right) + \mu\left[\left(\frac{\partial u}{\partial y}\right)^2 + \left(\frac{\partial w}{\partial y}\right)^2\right] + \sigma B_0^2\left[(u-U)^2 + w^2\right] + QC_0Ae^{-\frac{E}{RT}}, \tag{20}$$

where k is the thermal conductivity, c_p the specific heat at constant pressure, T the temperature of the fluid, μ the coefficient of viscosity, Q the heat of reaction, C_0 the initial concentration of reacting species, A the rate constant, R the universal gas constant. The first term on right hand side is for heat conduc-

tion, the second term for viscous dissipation, the third term for Joule heating and the fourth term for Arrhenius reaction.

The initial and boundary conditions for temperature are

$$t \leqslant 0: \quad T = T_0 \text{ for } 0 \leqslant y \leqslant h,$$
$$t > 0: \quad T = T_0 \text{ at } y = 0 \text{ and } T = T_0 \text{ at } y = h. \tag{21}$$

Following [30], the fluid thermal conductivity is assumed to vary exponentially with temperature such that

$$k(T) = k_0 e^{m(T-T_0)} \approx k_0[1 + m(T - T_0)], \tag{22}$$

where the parameter m may be positive for some fluids such as air or water vapor or negative for others like benzene.

Introducing the non-dimensional variable $\theta = \frac{E(T-T_0)}{RT_0^2}$, Eq. (20) becomes

$$Pr\frac{\partial\theta}{\partial\tau} = \frac{\partial}{\partial\eta}\left[(1+\delta\theta)\frac{\partial\theta}{\partial\eta}\right] + \lambda e^{\frac{\theta}{1+\varepsilon\theta}} + Pr\,Ec\left[\left\{\left(\frac{\partial u_1}{\partial\eta}\right)^2 + \left(\frac{\partial w_1}{\partial\eta}\right)^2\right\} + M^2\left\{(u_1-1)^2 + w_1^2\right\}\right], \tag{23}$$

where $Ec = \frac{Eu_0^2}{c_p RT_0^2}$ is the Eckert number which expresses the relationship between a flow's kinetic energy and enthalpy, $\lambda = \frac{QC_0Ah^2}{T_0^2 Ek_0} e^{-\frac{E}{RT_0}}$ the Frank-Kamenetskii parameter or reaction rate parameter, $\epsilon = \frac{RT_0}{E}$ the activation energy parameter, $\delta = \frac{mRT_0^2}{E}$ thermal conductivity variation parameter and $Pr = \frac{\rho\nu c_p}{k_0}$ the Prandtl number which is defined as the ratio of momentum diffusivity (kinematic viscosity) to thermal diffusivity.

The corresponding initial and boundary conditions are

$$\theta(\eta, 0) = 0 \text{ for } 0 \leqslant \eta \leqslant 1,$$
$$\theta(0, \tau) = 0 \text{ and } \theta(1, \tau) = 0 \text{ for } \tau > 0. \tag{24}$$

The analytical solution of fluid velocity (17) is used in Eq. (23), and the resulting differential equation subject to the MHD flow in a rotating system with initial and boundary conditions (24) is solved numerically with the help of MATLAB software package pdepe. For the analysis of heat transfer characteristics in the flow discussed above, energy equation is taken in which all the convective terms become equal to zero because plates of the channel are infinite in extent in x and z-directions. Therefore, the temperature distribution in the rotating channel is due to the heat generation by viscous and Joule dissipations and conduction through the fluid in the transverse direction. The Prandtl number (Pr) is chosen the values ranging from $0.72 \leqslant Pr \leqslant 2$ which are the most encountered fluids used in plasma physics, engineering, industries and nuclear power plant as coolant. $Ec = 0$ presents no Joule and viscous heating. In the absence of rotation ($K^2 = 0$), the present study reduces to the problem studied by Makinde and Franks [30]. In order to verify the accuracy of the present results, we have compared the results for the temperature profiles with those reported by Makinde and Franks [30]. These comparisons show excellent agreement (Fig. 10).

3.4. Effects of parameters on temperature profiles

Fig. 11 exhibits the time evolution of the temperature profiles across the channel for a fixed set of parameter values. The

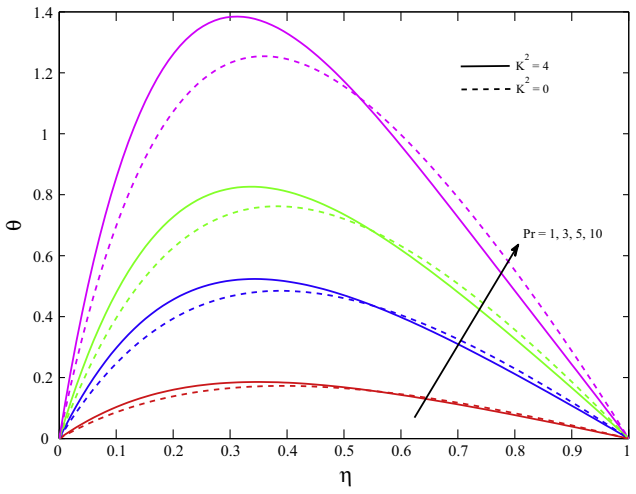

Figure 10 Temperature profiles for varying Pr when $M^2 = 1$, $\delta = 0.1$, $Ec = 1$, $\lambda = 0.1$ and $\varepsilon = 0.1$.

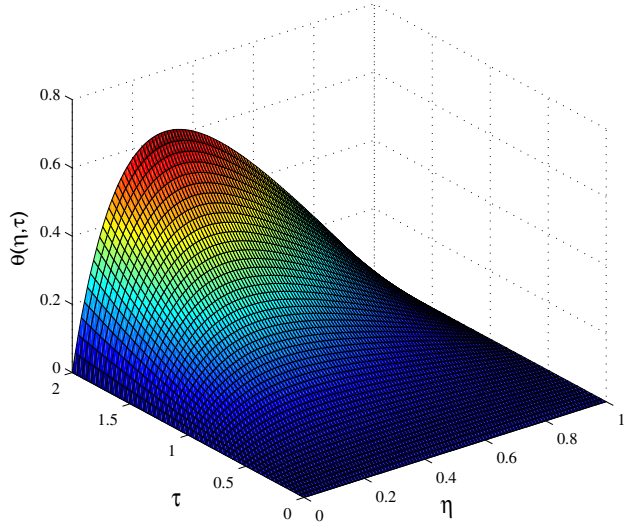

Figure 11 Temperature profiles across the channel with increasing time when $M^2 = 5, K^2 = 4, Pr = 0.71, Ec = 1, \delta = 0.1, \lambda = 0.1$ and $\varepsilon = 0.1$.

temperature increases from its zero value at the lower fixed plate to its maximum value at the center region of the channel. Fig. 12 depicts that the fluid temperature θ rises with an increase in either magnetic parameter M^2 or Frank-Kamenetskii parameter λ. A rise in magnetic field intensity (M^2) causes an increase in the fluid temperature within the channel. This may be explained as the effect of internal heating generation due to Joule dissipation. An increase in λ increases the internal heat generation within the channel due to exothermic reaction, leading to a rise in the fluid temperature.

Fig. 13 shows that fluid temperature θ increases as K^2 increases whereas it decreases with an increase in thermal conductivity variation parameter δ. As the rotation parameter increases, the Coriolis force increases which results in an increase in temperature profiles. As δ increases, the viscous heating effect decreases and hence the fluid temperature drops.

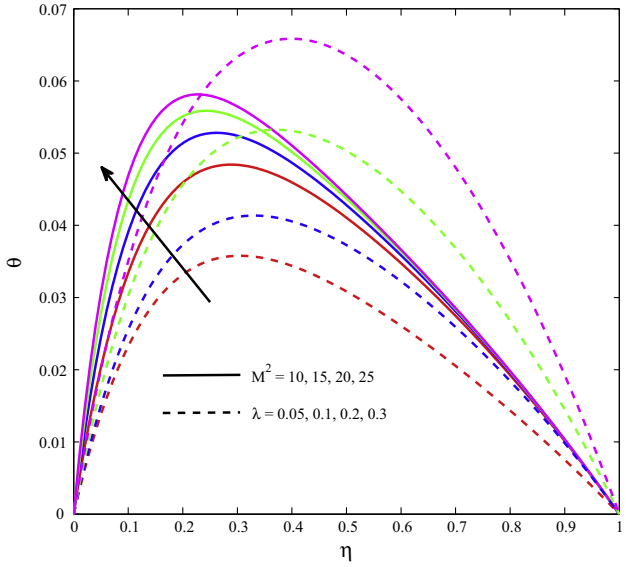

Figure 12 Temperature profiles for different M^2 and λ when $K^2 = 4, Pr = 0.71, Ec = 1, \delta = 0.1, \tau = 0.1$ and $\varepsilon = 0.1$.

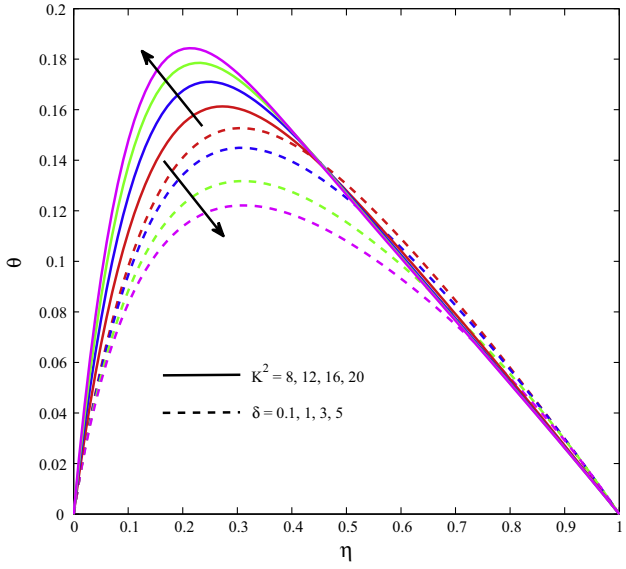

Figure 13 Temperature profiles for different K^2 and δ when $M^2 = 5, Pr = 0.71, Ec = 1, \lambda = 0.1, \tau = 0.1$ and $\varepsilon = 0.1$.

Fig. 14 demonstrates that the fluid temperature θ increases with an increase in either Prandtl number Pr or Eckert number Ec. Prandtl number defines the ratio of momentum diffusivity to thermal diffusivity for a given fluid. This may be attributed to the fact that as Pr increases, the fluid thermal diffusivity decreases, leading to accumulation of heat due to increasing viscous dissipation effect and hence fluid temperature rises the MHD reactive flow system. It is noted that small Prandtl number reactive fluids are more stable as compared to large Prandtl number reactive fluids. Eckert number Ec is the ratio of the kinetic energy of the flow system to the enthalpy differences. It represents the conversion of the kinetic energy into internal energy by work done against the reactive viscous fluid stresses. The positive values of Eckert number mean cooling of

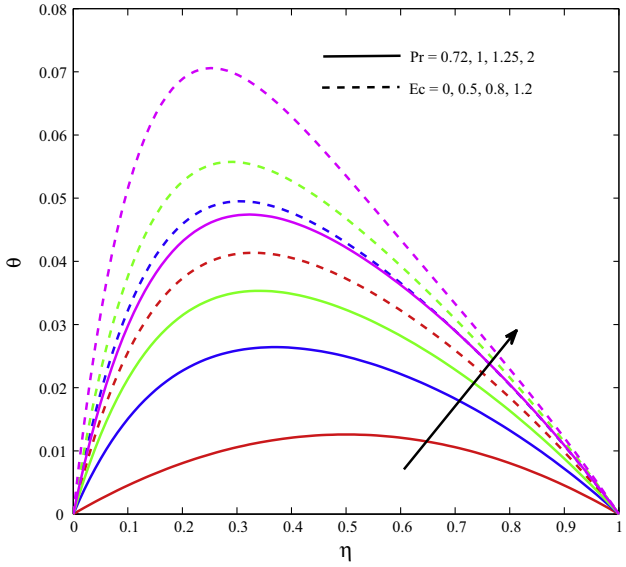

Figure 14 Temperature profiles for different Pr and Ec when $K^2 = 4, M^2 = 5, \lambda = 0.1, \delta = 0.1, \tau = 0.1$ and $\varepsilon = 0.1$.

the channel plates, i.e. loss of heat from the plates to the fluid. Hence, greater viscous dissipative heat causes a rise in the fluid temperature.

3.5. *Effects of parameters on rate of heat transfer*

Numerical results of the rate of heat transfer $-\theta'(0,\tau)$ at the lower plate $\eta = 0$ and the rate of heat transfer $-\theta'(1,\tau)$ at the upper plate $\eta = 1$ for several values of magnetic parameter M^2, Eckert number Ec, Prandtl number Pr and thermal conductivity variation parameter δ are presented in Figs. 15–18.

Fig. 15 shows that the rate of heat transfer $-\theta'(0,\tau)$ increases with an increase in either M^2 or time τ whereas the

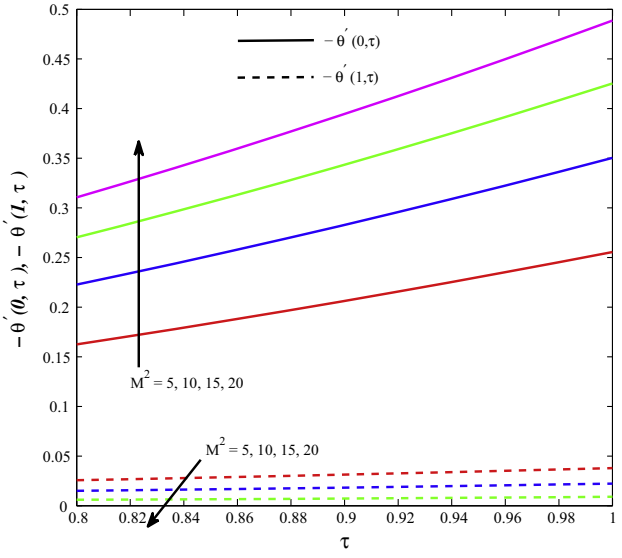

Figure 15 Rate of heat transfer $\theta'(0,\tau)$ and $\theta'(1,\tau)$ for different M^2 when $K^2 = 4, Pr = 0.71, Ec = 1, \delta = 0.1, \lambda = 0.1$ and $\varepsilon = 0.1$.

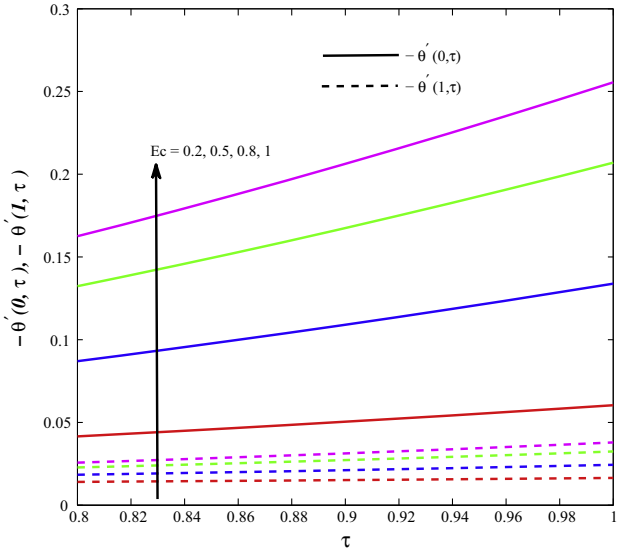

Figure 16 Rate of heat transfer $\theta'(0,\tau)$ and $\theta'(1,\tau)$ for different Ec when $K^2 = 4, Pr = 0.71, M^2 = 5, \delta = 0.1, \lambda = 0.1$ and $\varepsilon = 0.1$.

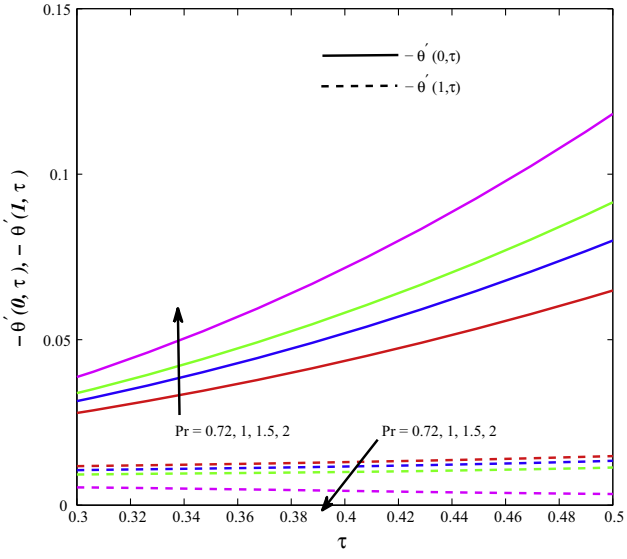

Figure 17 Rate of heat transfer $\theta'(0,\tau)$ and $\theta'(1,\tau)$ for different Pr when $K^2 = 4, M^2 = 5, \delta = 0.1, \lambda = 0.1$ and $\varepsilon = 0.1$.

rate of heat transfer $-\theta'(1,\tau)$ reduces as M^2 increases. It is clear that the rate of heat transfer is less near the moving plate in the presence of magnetic field. Fig. 16 shows that the rate of heat transfer $-\theta'(0,\tau)$ and $-\theta'(1,\tau)$ increases with an increase in either Ec or time τ. This can be attributed to the fact that as Eckert number or time increases, the dominance effect of temperature gradient increases, leading to an increase in the rate of heat transfer at both the plates. Fig. 16 shows that the rate of heat transfer $-\theta'(0,\tau)$ increases whereas the rate of heat transfer $-\theta'(1,\tau)$ reduces when Prandtl number Pr increases. This may be also explained by the fact that frictional forces become dominant at the stationary plate for increasing values of Prandtl number Pr and hence yield greater heat transfer rate.

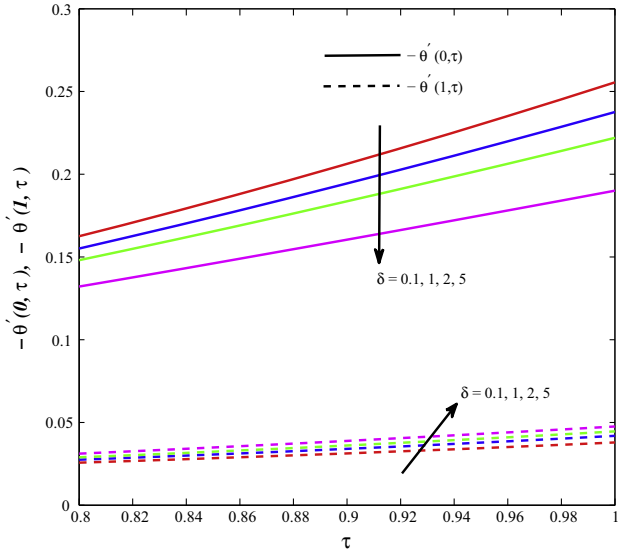

Figure 18 Rate of heat transfer $\theta'(0,\tau)$ and $\theta'(1,\tau)$ for different δ when $K^2 = 4, Pr = 0.71, M^2 = 5, Ec = 1, \lambda = 0.1$ and $\varepsilon = 0.1$.

Hence, Prandtl number can be used to control the rate of cooling in flow systems. Fig. 17 shows that the rate of heat transfer $-\theta'(0,\tau)$ decreases whereas the rate of heat transfer $-\theta'(1,\tau)$ increases with an increase in δ. As δ increases, the thermal conductivity of fluid enhances and hence heat can diffuse from the moving plate faster. As a result, the rate of heat transfer at the moving plate increases.

4. Conclusion

In this paper, a transient hydromagnetic Couette flow and heat transfer of a reactive viscous incompressible electrically conducting fluid between two infinitely long horizontal parallel plates in the presence of a uniform transverse magnetic field in a rotating system when one of the plate is set into uniform accelerated motion under Arrhenius reaction rate has been presented. A unified closed form analytical expressions for the velocity field and the shear stresses have been derived using the Laplace transform technique. The energy equation is solved numerically using MATLAB. Based on the graphical presentations, the following conclusions can be summarized as follows:

- The velocity of reactive viscous fluid within the channel has been significantly modified due to combined effects of magnetic field and rotation.
- The velocity of reactive viscous fluid within the channel is accelerated when time progresses.
- The temperature of reactive viscous fluid within the channel reduces due to increasing variable thermal conductivity while it enhances for increasing values of magnetic parameter or Frank-Kamenetskii or rotation or Eckert number.
- The rotation enhances the absolute value of the shear stresses at the lower plate.
- The shear stress due to the primary flow enhances whereas the shear stress due to the secondary flow reduces at the lower plate for increasing values of magnetic parameter.

- The rate of heat transfer at the lower plate enhances whereas the rate of heat transfer at the upper plate reduces as magnetic parameter increases.

References

[1] Y.S. Muzychka, M.M. Yovanovich, Unsteady viscous flows and Stokes' first problem, **Proc. IMECE 14301 (2006) 1–11.
[2] R.S. Nanda, H.K. Mohanty, Hydromagnetic flow in a rotating channel, Appl. Sci. Res. 24 (1970) 65–78.
[3] R.N. Jana, N. Datta, B.S. Mazumder, Magnetohydrodynamic Couette flow and heat transfer in a rotating system, J. Phys. Soc. Jpn. 42 (1977) 1034–1039.
[4] R.N. Jana, N. Datta, Hall effects on MHD Couette flow in a rotating system, Czech. J. Phys. 330 (1980) 659.
[5] G.S. Seth, R.N. Jana, M.K. Maity, Unsteady hydromagnetic Couette flow in a rotating system, Int. J. Eng. Sci. 20 (1982) 989–999.
[6] G.S. Seth, M.K. Maiti, MHD Couette flow and heat transfer in a rotating system, Ind. J. Pure Appl. Math. 13 (1982) 931–945.
[7] G.S. Seth, S.K. Ghosh, Effect of Hall current on unsteady hydromagnetic flow in a rotating channel with oscillating pressure gradient, Ind. J. Pure Appl. Math. 17 (6) (1986) 819–826.
[8] P. Chandran, N.C. Sacheti, A.K. Singh, Effect of rotation on unsteady hydromagnetic Couette flow, Astrophys. Space Sci. 202 (1993) 110.
[9] A.K. Singh, P. Chandran, N.C. Sacheti, Transient effects on magnetohydrodynamic Couette flow with rotation: accelerated motion, Int. J. Eng. Sci. 32 (1994) 133–139.
[10] S. Das, S.L. Maji, M. Guria, R.N. Jana, Unsteady MHD Couette flow in a rotating system, Math. Comput. Modell. 50 (2009) 1211–1217.
[11] S.K. Gosh, O. Anwar Bég, M. Narahari, Hall effects on MHD flow in a rotating system with heat transfer characteristics, Meccanica 44 (2009) 741–765.
[12] G.S. Seth, Md. S. Ansari, R. Nandkeolyar, Unsteady hydromagnetic Couette flow induced due to accelerated movement of one of the porous plates of the channel in a rotating system, Int. J. Appl. Math. Mech. 6 (7) (2010) 24–42.
[13] B.K. Jha, C.A. Apere, Combined effect of hall and ionslip currents on unsteady MHD couette flows in a rotating system, J. Phys. Soc. Jpn. 79 (2010) 104401 [9 pages].
[14] B.K. Jha, C.A. Apere, Time-dependent MHD Couette flow in a rotating system with suction/injection, Z. Angew. Math. Mech. 91 (10) (2011) 832–842.
[15] O. Anwar Bég, Lik Sim, J. Zueco, R. Bhargava, Numerical study of magnetohydrodynamic viscous plasma flow in rotating porous media with Hall currents and inclined magnetic field influence, Commun. Nonlin. Sci. Numer. Simulat. 15 (2010) 345–359.
[16] S. Das, B.C. Sarkar, R.N. Jana, Hall effects on MHD Couette flow in rotating system, Int. J. Comput. Appl. 35 (13) (2011) 22–30.
[17] B.K. Jha, C.A. Apere, Time-dependent MHD Couette flow of rotating fluid with Hall and ion-slip currents, Appl. Math. Mech. 33 (2012) 399–410.
[18] K.D. Singh, R. Pathak, Effect of rotation and Hall current on mixed convection MHD flow through a porous medium filled in a vertical channel in presence of thermal radiation, Ind. J. Pure Appl. Phys. 50 (2012) 77–85.
[19] D.S. Chauhan, R. Agrawal, Effects of Hall current on MHD Couette flow in a channel partially filled with a porous medium in a rotating system, Meccanica 47 (2012) 405–421.
[20] G.S. Seth, J.K. Singh, Effects of Hall current on unsteady MHD Couette flow of class-II in a rotating system, J. Appl. Fluid Mech. 6 (4) (2013) 473–484.
[21] S.K. Gosh, O. Anwar Bég, M. Narahari, A study of unsteady rotating hydromagnetic free and forced convection in a channel subject to forced oscillation under an oblique magnetic field, J. Appl. Fluid Mech. 6 (2) (2013) 213–227.
[22] G.S. Seth, B. Kumbhakar, R. Sharma, Unsteady hydromagnetic natural convection flow of a heat absorbing fluid within a rotating vertical channel in porous medium with Hall effects, J. Appl. Fluid Mech. 8 (4) (2015) 767–779.
[23] G.S. Seth, J.K. Singh, Mixed convection hydromagnetic flow in a rotating channel with Hall and wall conductance effects, Appl. Math. Model. (2015), http://dx.doi.org/10.1016/j.apm.2015.10.015.
[24] O.D. Makinde, On steady flow of a reactive variable viscosity fluid in a cylindrical pipe with an isothermal wall, Int. J. Numer. Meth. Heat Fluid Flow 17 (2) (2007) 187–194.
[25] N.S. Kobo, O.D. Makinde, Second law analysis for a variable viscosity reactive Couette flow under Arrhenius kinetics, Math. Probl. Eng. (2010) 1–15 278104.
[26] O.D. Makinde, O.O. Onyejekwe, A numerical study of MHD generalized Couette flow and heat transfer with variable viscosity and electrical conductivity, J. Magn. Magn. Mater. 323 (2011) 2757–2763.
[27] T. Chinyoka, O.D. Makinde, Analysis of transient generalized Couette flow of a reactive variable viscosity third-grade liquid with asymmetric convective cooling, Math. Comput. Model. 54 (2011) 160–174.
[28] D. Theuri, O.D. Makinde, Thermodynamic analysis of variable viscosity MHD unsteady generalized Couette flow with permeable walls, Appl. Comput. Math. 3 (1) (2014) 1–8.
[29] O.D. Makinde, Thermal analysis of a reactive generalized Couette flow of power law fluids between concentric cylindrical pipes, Eur. Phys. J. Plus 129 (2014) 2–9.
[30] O.D. Makinde, O. Franks, On MHD unsteady reactive Couette flow with heat transfer and variable properties, Cent. Eur. J. Eng. 4 (2014) 54–63.
[31] B.K. Jha, B.Y. Isah, I.J. Uwanta, Unsteady MHD free convective Couette flow between vertical porous plates with thermal radiation, J. King Saud Univ. – Sci. 27 (2015) 338–348.
[32] B.K. Jha, B. Aina, S. Isa, Fully developed MHD natural convection flow in a vertical annular microchannel: an exact solution, J. King Saud Univ. – Sci. 27 (2015) 253–259.
[33] A. Nayak, G.C. Dash, Magnetohydrodynamic couple stress fluid flow through a porous medium in a rotating channel, J. Eng. Thermophys. 24 (3) (2015) 283–295.
[34] K.R. Cramer, S.I. Pai, Magnetofluid Dynamics for Engineers and Applied Physicists, McGraw-Hill, New York, 1973.